

Supporting Information

Macroporous methacrylated hyaluronic acid cryogels of high mechanical strength and flow-dependent viscoelasticity

Burak TAVSANLI, and Oguz OKAY*

Department of Chemistry, Istanbul Technical University, 34469 Maslak, Istanbul, Turkey

Determination of compressive fracture stress of the cryogels

The compressive fracture stress values of the cryogels were calculated from the maxima of true stress–strain curves, where the true stress σ_{true} is the force per cross-sectional area of the deformed gel specimen and, assuming isotropic deformation during compression, it is related to the nominal stress σ_{nom} by $\sigma_{\text{true}} = \lambda \sigma_{\text{nom}}$, where λ is the deformation ratio, i.e., $\lambda = 1 - \varepsilon$. For instance, Figures S2a, S2b show stress-strain curves of two cryogel samples as the dependences of the nominal σ_{nom} (solid black curves) and true stresses σ_{true} (dashed blue curves) on the strain ε . Although the nominal stress σ_{nom} continuously increases with increasing strain up to around complete compression, the corresponding $\sigma_{\text{true}} - \varepsilon$ plots pass through maxima at 96-99% compressions. This behavior is a result of the gel samples with microscopic cracks still supporting the stress and nonisotropic deformation of gel samples under large strain. Therefore, the fracture nominal stress σ_f and strain ε_f at failure were calculated from the maxima in $\sigma_{\text{true}} - \varepsilon$ plots, as indicated by the red arrows in the figures. The corrected $\sigma_{\text{nom}} - \varepsilon$ plots are shown in the figures by thick black curves. Thus, for the samples in Figures S2a and S2b, the fracture stresses σ_f are 3.6 and 2.5 MPa, respectively.

Table S1. Gel fraction W_g , water content H₂O %, weight q_w and volume swelling ratios q_v , total porosity P , fracture stress σ_f , and Young's modulus E of HA cryogels.^a

Meth %	DMAA wt%	W_g	H ₂ O %	q_w	q_v	P %	σ_f / MPa	E / kPa	σ_f / MPa	E / kPa
							Dry state		Swollen state	
4	0.5	0.99	99	140 (6)	1.25	99.5	0.3	8 (3)	2.6 (0.2)	0.32 (0.07)
14	0.5	0.99	99	117 (4)	1.19	99.4	0.2	15 (5)	2.3 (0.7)	0.39 (0.04)
25	0.5	1.00	99	91 (8)	1.14	99.3	0.17	21	1.5 (0.2)	0.56 (0.2)
4	1	1.00	99	83 (7)	1.14	99.2	0.54	24 (3)	2.5 (0.2)	0.59 (0.2)
14	1	0.98	98	66 (6)	1.08	99.1	0.48	34 (6)	1.9 (0.2)	0.67 (0.2)
25	1	1.00	98	60 (8)	1.04	99.0	0.27	46 (5)	1.8	0.67 (0.02)
4	2	0.99	98	54 (3)	1.15	99.8	1.6 (0.4)	50 (10)	1.1 (0.1)	0.6
14	2	0.97	98	41 (3)	1.12	98.5	1.3	61 (18)	1.0	0.7 (0.1)
25	2	1.00	97	39 (1)	1.09	98.5	0.9 (0.1)	121 (26)	0.6 (0.1)	1.1 (0.2)
4	5	0.98	96	26 (2)	1.03	97.8	3.6 (0.6)	128 (22)	0.5	1.3 (0.3)
14	5	0.94	95	22 (2)	1.04	97.3	2.9 (0.6)	240 (8)	0.3	1.6 (0.8)
25	5	0.87	95	22 (2)	1.06	97.2	2.4 (0.2)	370 (70)	0.2	3.38 (0.1)

^a Standard deviations are given in parenthesis while for H₂O %, W_g , and q_v , they are less than 0.2, 5, and 5%, respectively.

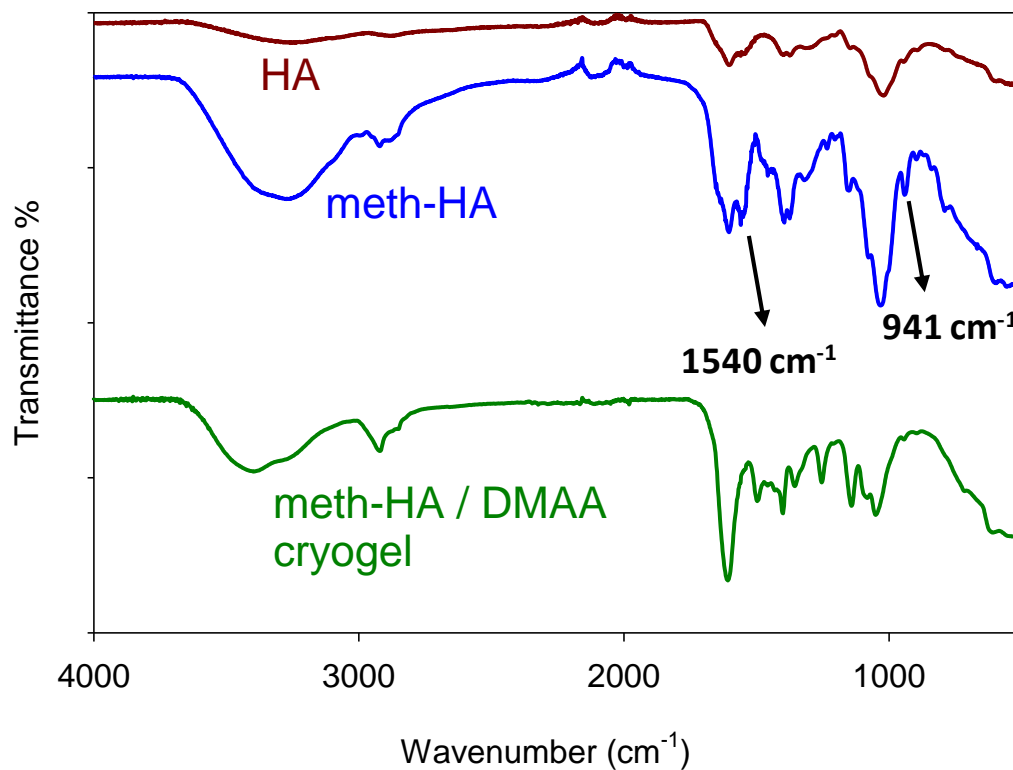


Figure S1. (a): FTIR-ATR spectra of native HA, meth-HA, and freeze-dried HA cryogel. Meth-HA was prepared at a GM/HA molar ratio of 6. DMAA content of the cryogel = 0.5 wt %. The spectra were recorded on a Nicolet Nexus 6700 spectrophotometer using a single-bounce diamond ATR accessory equipped with a liquid nitrogen cooled mercury–cadmium–telluride (MCT) detector. 64 interferograms at 4 cm⁻¹ resolution were co-added to generate each spectrum.

The appearance of the peaks at 941 and 1540 cm⁻¹ in the spectrum of meth-HA indicates the presence of the methacrylate carbon-to-carbon double bonds that disappear after cryogelation indicating incorporation of meth-HA into the cryogel network.

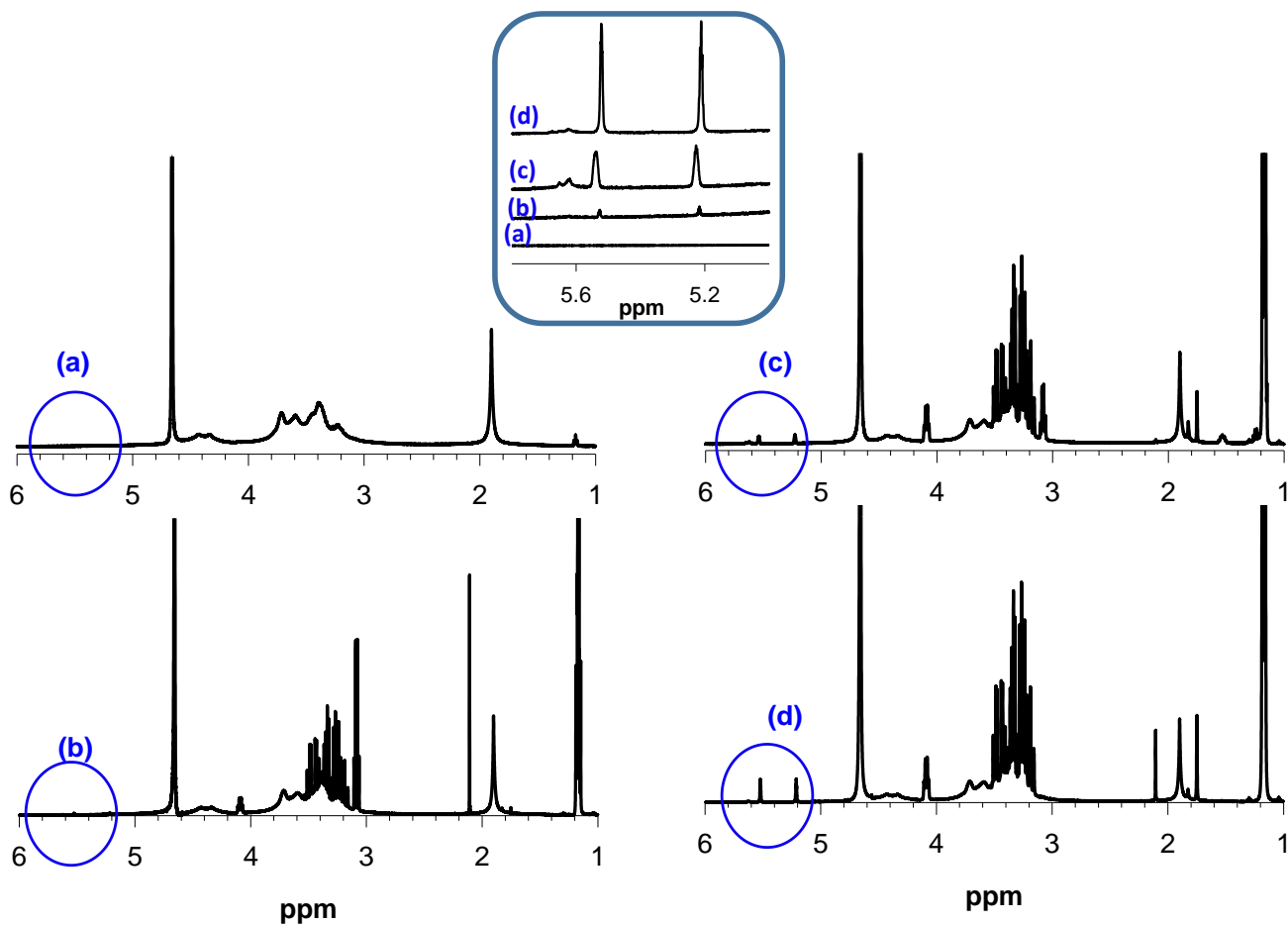


Figure S1. (b): ^1H NMR spectra of native HA (a) and meth-HA prepared at GM/HA molar ratios of 6 (b), 24 (c), and 49 (d). The region between 5 and 6 ppm is highlighted in circles. The inset is a zoom-in of the 5.0–5.8 ppm region of the spectra. The peaks at 5.5 and 5.2 ppm are indicative of methacrylate groups. The degree of methacrylation was determined by integration of the methyl peak of HA at 1.9 ppm and the methacrylate peaks. The methacrylation degrees are 4, 14, and 25% for b, c, and d, respectively.

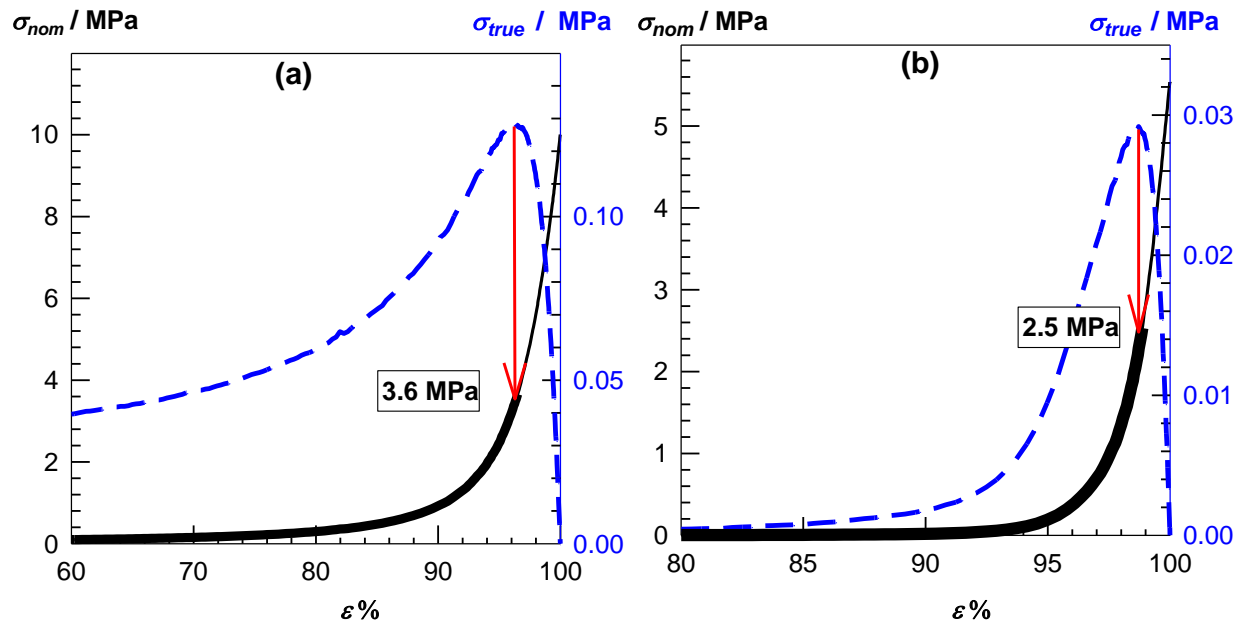


Figure S2. Typical stress-strain curves of cryogels under compression as the dependences of nominal σ_{nom} (solid black curves) and true stresses σ_{true} (dashed blue curves) on the strain ϵ . The thick black curves are corrected $\sigma_{nom} - \epsilon$ plots. **(a):** Freeze-dried HA cryogel formed at 4% Meth and 5 wt % DMAA. **(b):** Swollen HA cryogel formed at 4% Meth and 0.5 wt % DMAA.

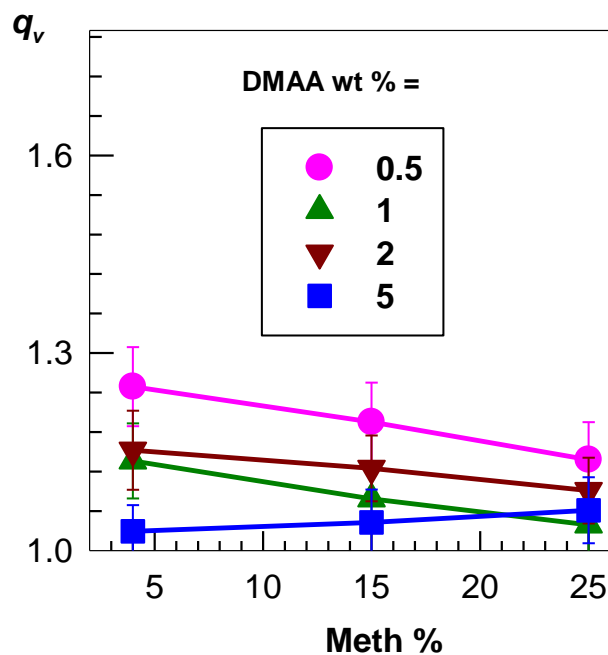


Figure S3. Equilibrium volume swelling ratio q_v of HA cryogels in water shown as a function of Meth of HA. DMAA contents are indicated.

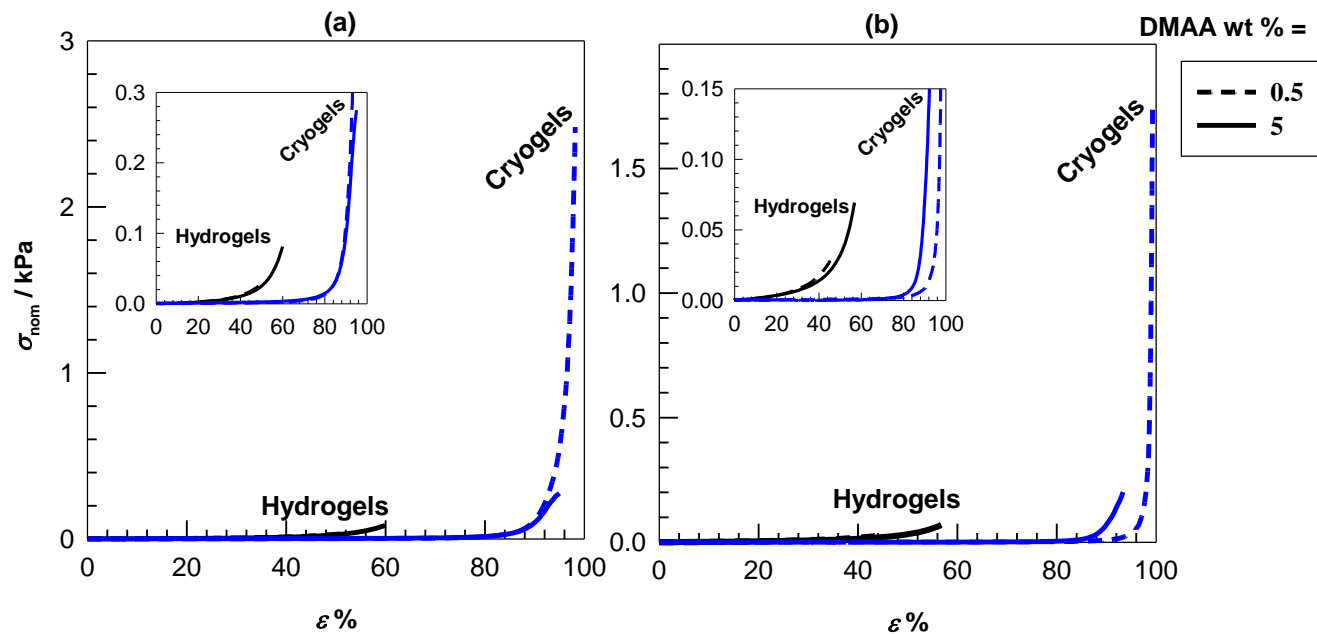


Figure S4. Stress-strain curves of swollen HA cryogels (blue curves) and the corresponding hydrogels prepared at 23 ± 2 °C (black curves). The insets are zoom-in of low strain region. Meth of HA = 14 (a) and 25% (b). DMAA wt % indicated.

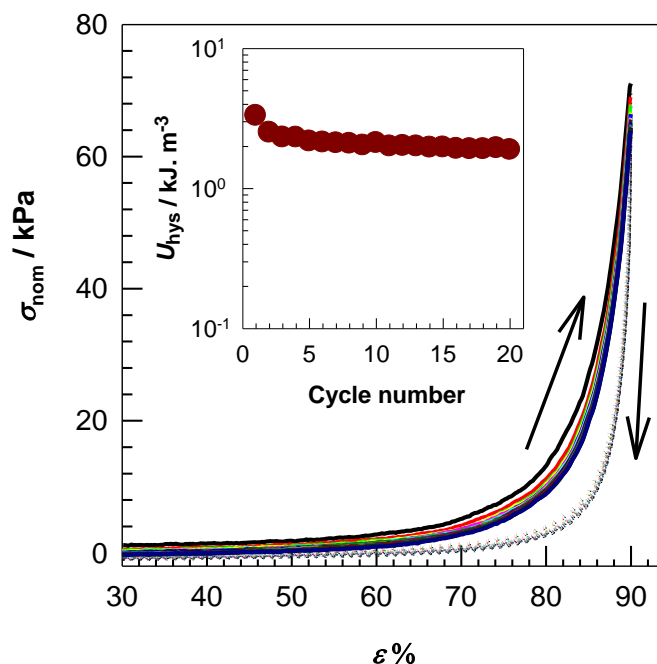


Figure S5. 20 successive loading and unloading cycles conducted on a cryogel specimen prepared at 4% Meth and 0.5 wt % DMAA. Strain rate = $1 \text{ mm} \cdot \text{min}^{-1}$. The loading and unloading curves are shown by the solid and dotted curves, respectively. The inset shows the hysteresis energy U_{hys} , i.e., the area between the loading and unloading curves plotted against the number of cycles.

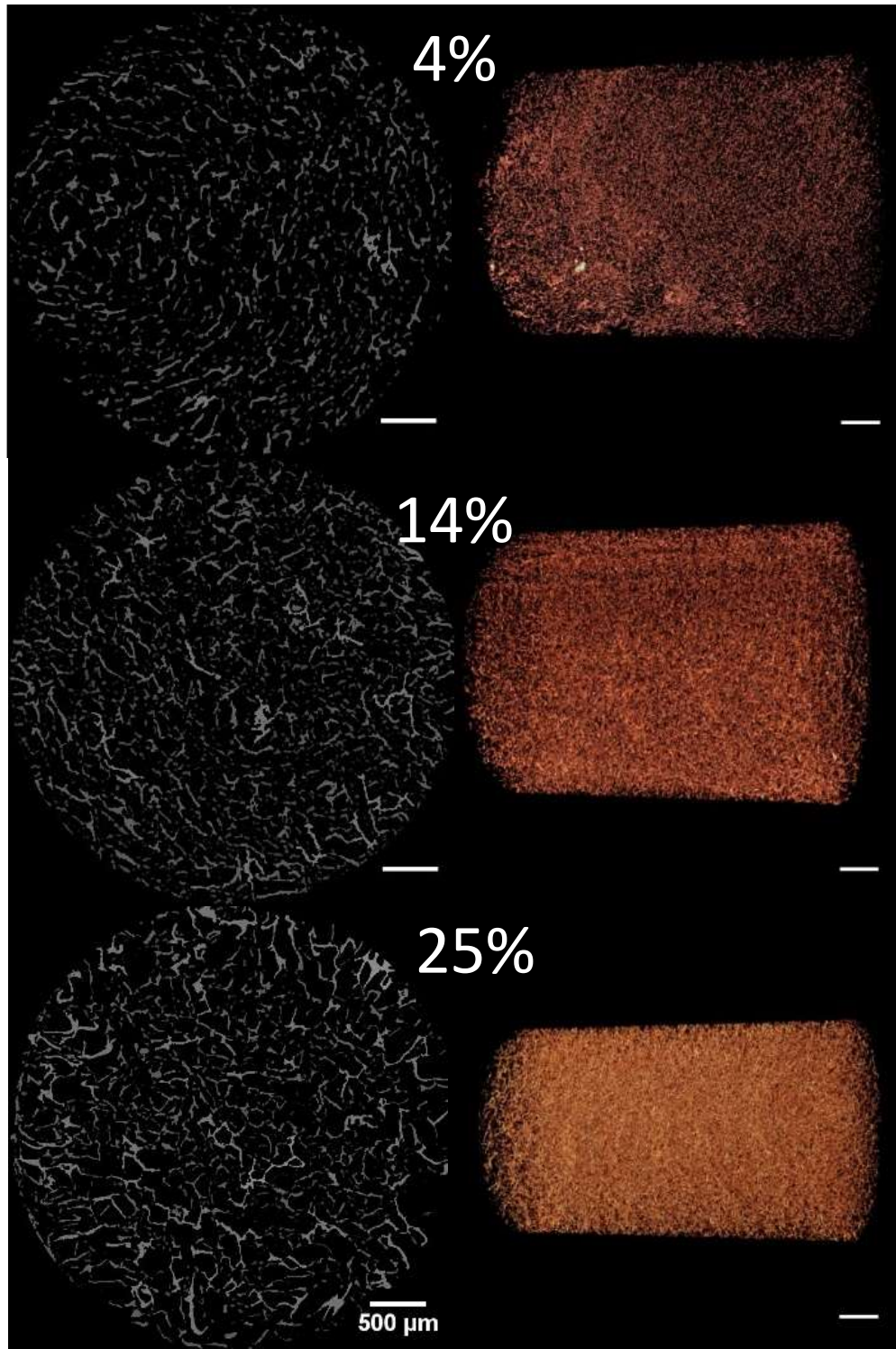


Figure S6. 2D (left) and 3D μ -CT images (right) of cryogels formed 5 wt % DMAA and at various Meth of HA as indicated. Scale bars are 0.5 mm.

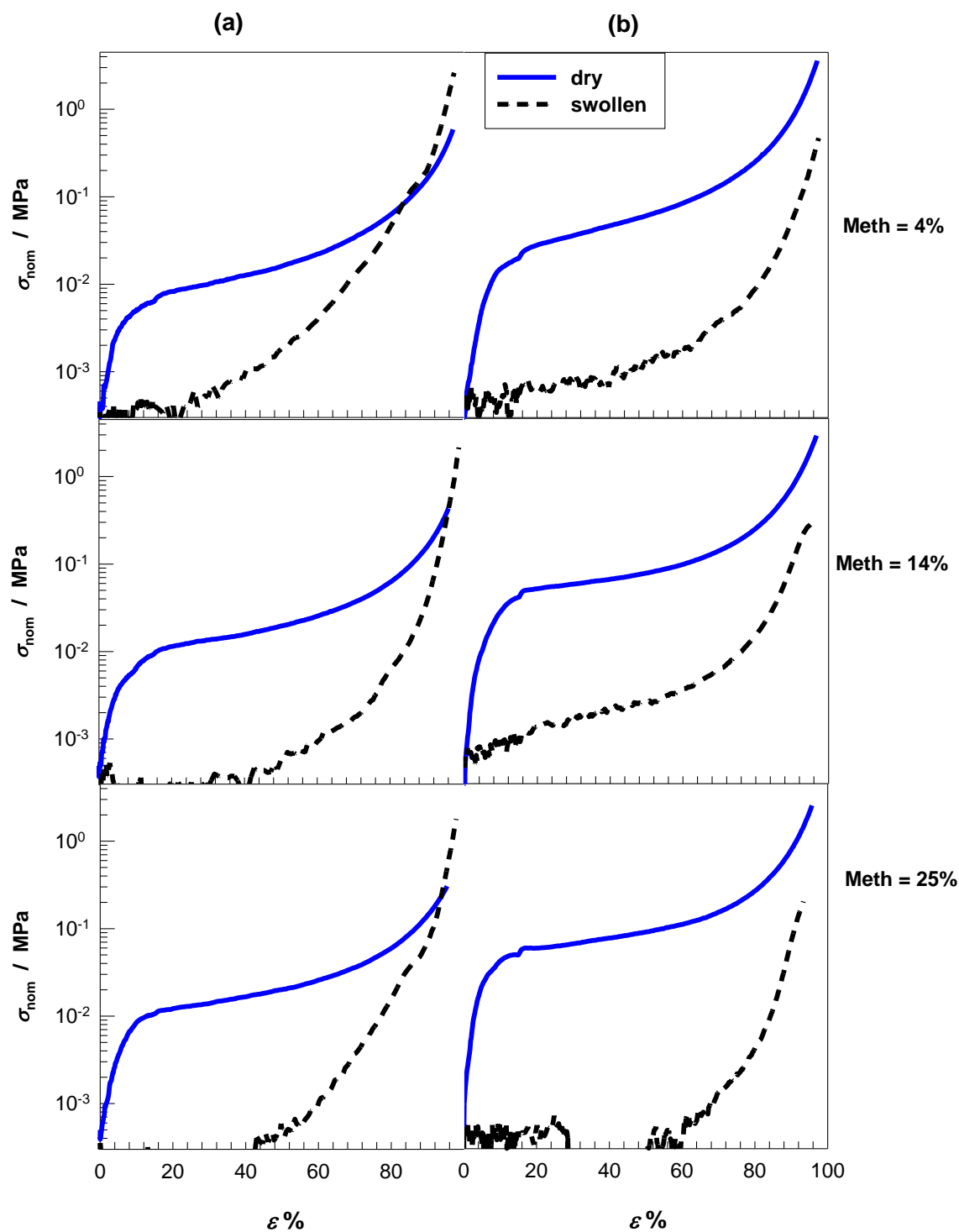


Figure S7. Stress-strain curves of freeze-dried (solid blue curves) and swollen HA cryogels (dashed black curves) formed at 1 (a) and 5 wt % DMAA (b). Meth of HA indicated.